Collisional frequency shifts and line broadening in the cryogenic deuterium maser

E. Tiesinga
Department of Physics, Eindhoven University of Technology, 5600 MB Eindhoven, The Netherlands

S. B. Crampton
Department of Physics, Williams College, Williamstown, Massachusetts 01267

B. J. Verhaar and H. T. C. Stoof
Department of Physics, Eindhoven University of Technology, 5600 MB Eindhoven, The Netherlands
(Received 14 December 1992)

We study the spin-exchange frequency shifts and line broadening of the deuterium maser in the temperature range from 0 to 10 K. We consider both a version operating on the β-ϵ transition at $B=3.0\ \mu$T and one operating on the β-δ transition at $B=3.9$ mT. For the first transition, a comparison is made with our earlier results based on the degenerate-internal-states approximation and its first-order corrections [E. Tiesinga, H. T. C. Stoof, B. J. Verhaar, and S. B. Crampton, Physica B **165&166**, 19 (1990)]. We find cusp structures due to channel thresholds and also resonance structures, both of which disappear almost completely after thermal averaging in the temperature range considered.

PACS number(s): 42.52.+x, 34.90.+q, 67.65.+z

I. INTRODUCTION

Atomic-hydrogen masers have been developed to study the hyperfine structure of all three hydrogen isotopes [1–3], but only hydrogen (H) has been used for precision measurements other than hyperfine-structure determinations near room temperature [4]. The radioactivity and relative scarcity of tritium severely limit its use. The lower deuterium (D) hyperfine frequency ($\approx$327 MHz) relative to the hydrogen frequency ($\approx$1420 MHz) makes it difficult to provide a stable rf-cavity Q value high enough for D-maser oscillation using a room-temperature cavity [3]. Of the two D transitions that have frequency minima at some magnetic field, the β-ϵ transition (adopting the conventional notation $\alpha\beta\gamma\delta\epsilon\zeta$ in order of increasing energy; see Fig. 1) is contaminated by the α-δ transition detuned by only 40 Hz, while the β-δ transition requires a stable and homogeneous 3.9-mT field, which is difficult to provide over the large experimental volumes used near room temperature [3].

Recent pulsed magnetic-resonance experiments on atomic deuterium gas near 1 K by Hardy and co-workers [5–7] suggest that D-maser oscillation can be achieved at low temperatures. Lifetimes against recombination were as long as 30 min, despite the tendency of D to dissolve in the liquid-helium film coating the experimental cell. The Q value of their superconducting rf cavity is high enough for D-maser oscillation using a state-selected atomic beam like those used in several low-temperature H-maser designs [8–10]. Uniform and stable magnetic fields near 3.9 mT can be maintained by superconducting magnetic shielding. Investigations of electron-spin-exchange collisions [11–15] in the D maser would be interesting in view of the current disagreement between experiments measuring collisional frequency shifts in H masers and theoretical predictions of the shifts due to hyperfine-structure effects during electron-exchange collisions [16,17]. Including such effects predicts collisional frequency shifts that are not canceled by cavity-pulling effects [18]. Moreover, they have potentially distinctive signatures because of their dependence on the H-level populations. Reanalysis of the earliest room-temperature experiment [19] in terms of these signatures to measure the hyperfine-induced shifts reveals a discrepancy of about 2 standard deviations. A more recent room-temperature experiment was designed to be particularly sensitive to the density-dependent frequency shifts proportional to the sum of the populations of the two H lev-

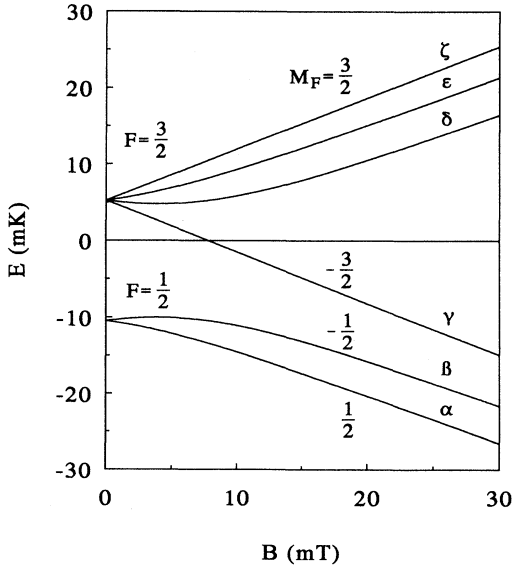

FIG. 1. Energies of the deuterium hyperfine states as a function of magnetic field.

els coupled by the oscillation [20]. Theory fails by 6 standard deviations to account for the magnitude of the measured shifts, which even have an opposite algebraic sign. Preliminary attempts [6] to measure frequency shift and broadening cross sections at cryogenic temperatures also disagree with theory by several standard deviations. In all three experiments the measured shifts are so small relative to the resonance linewidths and other sources of frequency shifts that it is difficult to estimate whether there may be contributions that only mimic the signature of the hyperfine-induced collisional shifts. Consequently, it would be interesting to compare theory to experiment in a related system in which both the theoretical predictions and competing systematic effects may be different. For this reason, we have calculated the hyperfine-induced frequency shifts for both the β-ϵ and β-δ transitions in a D maser. A preliminary report on part of the present work was presented previously [21]. It was restricted to the β-ϵ transition and was based on the degenerate-internal-states (DIS) approximation and its first-order correction. In the present paper, we also carry out full coupled-channel (CC) calculations. In Sec. II the method of calculation is explained. The frequency shift and broadening cross sections of the β-ϵ maser are studied in Sec. III. The appearance of cusps and resonances in the calculated quantities is discussed in some detail. In Sec. IV we discuss the β-δ maser and in Sec. V we present some conclusions.

II. METHOD

Our starting point is the time evolution of the single-atom spin-density matrix of an ensemble of deuterium atoms undergoing two-body spin-exchange collisions, which may be obtained [17] from the quantum-mechanical Bogoliubov-Born-Kirkwood-Yvon (BBGKY) hierarchy:

$$\left.\frac{d}{dt}\rho_{\kappa\kappa'}\right|_{\text{coll}} = \rho_{\kappa\kappa'} n \sum_{\nu} G_{\nu}\rho_{\nu\nu} \equiv \rho_{\kappa\kappa'}(i\Delta\omega_c - \Gamma_c) \ . \tag{1}$$

Here, n is the density, the summation is over all spin hyperfine states, and κ and κ' are the hyperfine states involved in the maser transition. The quantities $\Delta\omega_c$ and Γ_c are the collisional frequency shift and line broadening, respectively. The rate-constant-like quantities G_ν contain information on the spin-exchange collisions in the form of S-matrix elements:

$$G_{\nu} = \left\langle v \sum_{l} (2l+1) \sum_{\lambda} c_{\kappa\kappa'\lambda\nu} \frac{\pi}{k^2} \left[S^{l}_{\{\kappa\lambda\},\{\kappa\nu\}}(k) S^{l*}_{\{\kappa'\lambda\},\{\kappa'\nu\}}(k) - \delta_{\{\kappa\lambda\},\{\kappa\nu\}}\delta_{\{\kappa'\lambda\},\{\kappa'\nu\}} \right] \right\rangle_{\text{th}} ,$$

$$c_{\kappa\kappa'\lambda\nu} = \sqrt{(1+\delta_{\kappa\lambda})(1+\delta_{\kappa\nu})(1+\delta_{\kappa'\lambda})(1+\delta_{\kappa'\nu})} \ , \tag{2}$$

with $v = \hbar k/\mu$ the relative velocity of the atoms in the initial state, k the corresponding wave number, $\delta_{\mu\nu}$ the Kronecker delta, and the large angular brackets denoting a thermal average. Greek indices stand for hyperfine states and l is the orbital angular-momentum quantum number. The summation over m_l has already been carried out. The S^l-matrix elements describe the spin-exchange transition amplitude between spin states $\{\alpha\beta\}$ for a fixed value of l. In view of Fermi-Dirac statistics the two-particle (anti)symmetrized spin states are correlated with odd (even) l.

The S-matrix elements follow from the Schrödinger equation for a D+D collision, where the Hamiltonian includes intra-atomic hyperfine-interaction terms as well as interatomic singlet and triplet potentials as described in Refs. [22] and [23]. These potentials differ slightly from those of our previous papers on the collisional effects in the H maser [16,17] and the D maser [21]. However, only minor changes are expected for the final cross sections, taking into account the values of the singlet and triplet scattering lengths for both H+H and D+D, which all change by less than 1%.

Nonadiabatic corrections to the adiabatic Born-Oppenheimer approximation are taken into account by using the reduced deuterium atomic mass in the D+D Schrödinger equation. This procedure can be justified in the same way as for H+H scattering [16,17].

III. THE β-ϵ MASER

The frequency shift and line broadening due to spin-exchange collisions are directly given by Eq. (1). We rewrite this equation in terms of the frequency-shift cross sections λ_i and the line-broadening cross sections σ_i:

$$\Delta\omega_c = n\langle v\rangle_{\text{th}}[\bar{\lambda}_0(\rho_{\epsilon\epsilon}-\rho_{\beta\beta}) + \bar{\lambda}_1(\rho_{\epsilon\epsilon}+\rho_{\beta\beta}) + \bar{\lambda}_2\rho_{\alpha\alpha} + \bar{\lambda}_3\rho_{\gamma\gamma} + \bar{\lambda}_4\rho_{\delta\delta} + \bar{\lambda}_5\rho_{\zeta\zeta}] \ , \tag{3}$$

$$\Gamma_c = n\langle v\rangle_{\text{th}}[\bar{\sigma}_0(\rho_{\epsilon\epsilon}-\rho_{\beta\beta}) + \bar{\sigma}_1(\rho_{\epsilon\epsilon}+\rho_{\beta\beta}) + \bar{\sigma}_2\rho_{\alpha\alpha} + \bar{\sigma}_3\rho_{\gamma\gamma} + \bar{\sigma}_4\rho_{\delta\delta} + \bar{\sigma}_5\rho_{\zeta\zeta}] \ , \tag{4}$$

with the thermally averaged quantities

$$\bar{\lambda}(T) = \langle v\lambda(E)\rangle / \langle v\rangle_{\text{th}} \ , \tag{5}$$

$$\bar{\sigma}(T) = \langle v\sigma(E)\rangle / \langle v\rangle_{\text{th}} \ , \tag{6}$$

with $E = \frac{1}{2}\mu v^2$ the center-of-mass collision energy.

In Fig. 2 the results of CC calculations are shown as a function of collision energy for the four cross sections λ_0, λ_1, λ_2, and λ_4 of the β-ϵ maser at $B = 3.0$ μT. The remaining cross sections are omitted for clarity because they approximately satisfy $\lambda_2 = -\lambda_3/2 = \lambda_5$, which is exact in the DIS approximation at $B = 0$ T, as discussed

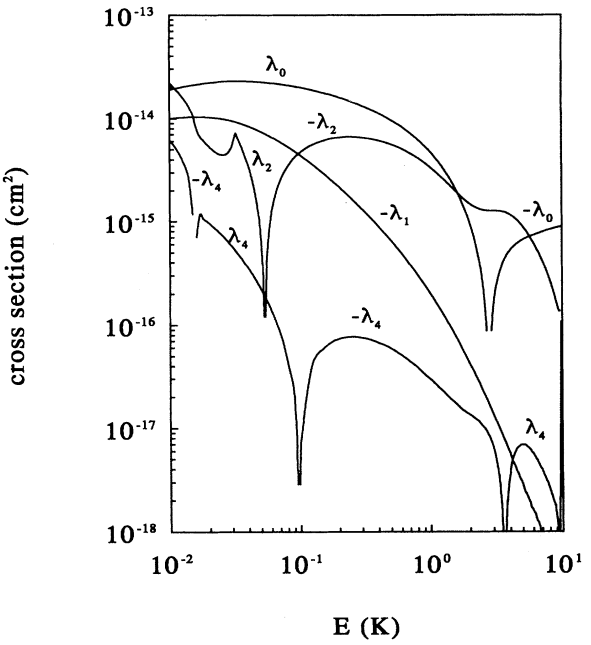

FIG. 2. Full coupled-channel results of frequency-shift cross sections for the β-ϵ maser as a function of collision energy E. Negative values of λ_i are plotted $-\lambda_i$.

below. It turns out that the agreement with our preliminary results in Ref. [21] is good, the discrepancies being generally less than 1%. One exception is connected with the cusplike discontinuities in λ_2 and λ_4 at low energies, to which we return below. Another exception is the quantity λ_1 in the higher part of the energy interval considered in Fig. 2, where it is very small.

The calculations in Ref. [21] were not based on full CC calculations, but instead on the DIS approximation and its first-order corrections. The DIS approximation is based on the assumption that the hyperfine splitting can be neglected in the calculation of the S-matrix elements in Eq. (2). This offers the possibility to express the latter in singlet and triplet scattering phase shifts, which are easily obtainable by means of an elastic scattering calculation:

$$S^{l(\mathrm{DIS})}_{\{\gamma\delta\},\{\alpha\beta\}}-\delta_{\{\gamma\delta\},\{\alpha\beta\}}=(\langle\{\gamma\delta\}|e^{2i\delta^l_0}P_0+e^{2i\delta^l_1}P_1|\{\alpha\beta\}\rangle -\delta_{\{\gamma\delta\},\{\alpha\beta\}})d^l_{\{\gamma\delta\},\{\alpha\beta\}}\ ,$$
$$d^l_{\{\gamma\delta\},\{\alpha\beta\}}=(k_{\{\gamma\delta\}}k_{\{\alpha\beta\}}/\bar{k}^2)^{l+1/2}\ , \tag{7}$$

P_0 (P_1) standing for a projection operator projecting on the singlet (triplet) subspace, $k_{\{\alpha\beta\}}$ and $k_{\{\gamma\delta\}}$ the initial and final wave numbers, and $\bar{k}$ and average wave number determined by $\bar{k}^2=(k^2_{\{\gamma\delta\}}+k^2_{\{\alpha\beta\}})/2$. The physical significance of the DIS approximation is illustrated by Eq. (7). The hyperfine interactions are responsible for the spin structure of the initial and final states $\{\alpha\beta\}$ and $\{\gamma\delta\}$, respectively, but are neglected during the collision. As pointed out in Ref. [21], introducing this approximation and neglecting the small influence of the magnetic field on the spin states, one finds λ_1 and λ_4 to be zero, while $\lambda_2=-\lambda_3/2=\lambda_5$, i.e.,

$$\Delta\omega_c=n\langle v\rangle[\bar{\lambda}_0(\rho_{\epsilon\epsilon}-\rho_{\beta\beta})+\bar{\lambda}_2(\rho_{\alpha\alpha}+\rho_{\xi\xi}-2\rho_{\gamma\gamma})]\ . \tag{8}$$

Finite values of λ_1 and λ_4 can be obtained by treating the influence of the hyperfine splitting on the collision in first order. In classical terms, we thus take into account the finite hyperfine precession angles of the electronic and nuclear spins during the collision. As pointed out in Ref. [24], a first-order Born-type treatment of the hyperfine interactions in a collision leads to a divergent space integral. A more subtle approach, derived in the same paper, replaces the spatial integral by one over a finite volume enclosing the interatomic interaction region, supplemented by an integral over the surface of this volume. The result is a correction of the form

$$\Delta S^l_{\{\gamma\delta\},\{\alpha\beta\}}=-\langle\{\gamma\delta\}|(P_1-P_0)(V^{\mathrm{hf}}-\epsilon)(P_1-P_0)|\{\alpha\beta\}\rangle d^l_{\{\gamma\delta\},\{\alpha\beta\}}\Delta^l(\bar{k})\ , \tag{9}$$

with V^{hf} the sum of the two hyperfine-interaction terms for the two atoms and ϵ the average hyperfine energy of the initial and final two-atom spin states. Equation (9) has the form of a simple spin matrix element multiplied by a quantity Δ^l computable by elastic scattering calculations:

$$\Delta^l(k)=\frac{1}{4i}\frac{m}{2\hbar^2k^2}\left[k\int_0^{r_0}(u^l_0-u^l_1)^2dr+\tfrac{1}{2}(S^l_0-S^l_1)^2W\left[O^l(kr),\frac{\partial}{\partial k}O^l(kr)\right]_{r=r_0}\right]\ , \tag{10}$$

where m is the deuterium mass, W is a Wronskian, O^l is a Hankel-like free outgoing wave with asymptotic behavior $e^{i(kr-l\pi/2)}$, and the DIS singlet (triplet) radial wave functions u^l_0 (u^l_1) are normalized so as to have the outgoing part $-S^l_S O^l$ with $S^l_S=e^{2i\delta^l_S}$. Note that the intermediate Eqs. (10) and (11) in Ref. [16], as well as (53) and (54) in Ref. [17], should contain an additional overall minus sign on their right-hand sides to be in agreement with the further equations and the final calculated cross sections in the same paper.

The above agreement of our present full CC calculations with the DIS (plus first order corrections) results in Ref. [21] confirms the validity of the previous simplified approach for systems as H+H and D+D. It is of interest to point out that the situation is completely different for the frequency shifts in the cesium atomic fountain, in which case the first-order corrections turn out to be so large that the unitarity limit is violated [25]. Also, in our previous work on Na+Na cold-atom collisions [26] we have found a similar breakdown of the

simplified approach. As noticed in Ref. [16], a DIS plus first-order corrections approach is not able to describe the cusps occurring in the energy dependence of some of the cross sections due to threshold effects. Whereas the exact S-matrix elements are analytic functions of each of the channel wave numbers, a nonalytic dependence appears as soon as the channel wave numbers—and particularly that of the channel that opens up at the threshold considered—are expressed in the collision energy. The resulting nonanalytic dependence on energy does not follow from a DIS plus first-order corrections approach. In this connection it is interesting to note that the cusps are absent in λ_0 and λ_1. This is understandable on the basis of the Wigner threshold law [27], which predicts a discontinuous energy derivative of S-matrix elements only for $l=0$. Indeed, it follows from Eqs. (2) and (5) and the fermion character of the D atoms that only odd partial waves contribute to λ_0 and λ_1.

In contrast with the H maser (for $B=0$), where inelastic S-matrix elements do not contribute to the collisional frequency shifts and broadenings for symmetry reasons, inelastic contributions are significant for the D maser. It turns out that, for low energies, σ_0, σ_1, and σ_2 are the only rates in which these inelastic contributions are important. For higher energies, σ_0 is completely determined by them, while inelastic components in other cross sections are negligible.

The cross sections in Fig. 2 have been obtained by summing over partial waves as indicated in Eq. (2). It is of interest to point out that individual partial-wave contributions contain a resonance structure that is almost invisible in the total sum. In Fig. 3 the partial-wave contributions to λ_2 as a function of collision energy are shown. The calculations have been continued up to energies of $E/k_B=100$ K since, later on, temperatures $T\leq 10$ K will be of interest and energies several times k_BT are needed for convergence of the thermal averaging. We see two clear resonance structures. One occurs for $l=6$ at 9.9 K.

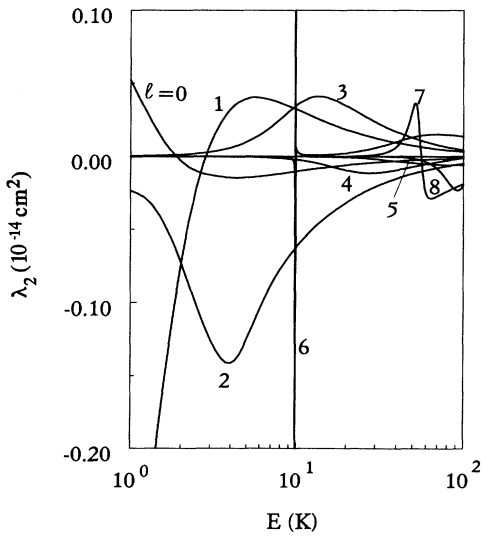

FIG. 3. Partial-wave contributions to λ_2 as a function of energy showing resonances for $l=6$ and 7.

Actually, it consists of three overlapping resonances with comparable widths that are only one hyperfine splitting apart. A similar resonance structure is seen for $l=7$ at 60 K.

The origin of the resonances can be understood in terms of an extrapolation of singlet bound states into the continuum. Treating l as a continuous variable (as in Regge theory [28]), the energy of a vibrational level v can be traced as a function of $l(l+1)$. Starting with an $l=0$ rotational bound state and increasing l continuously, the bound-state energy obtained by solving the radial equation increases until the threshold is reached. Above threshold, following Ref. [29], we determine for each fixed value of l the energy where the phase shift changes by π. In Fig. 4 we give the "trajectories" in the E-versus-$l(l+1)$ plane for the $v=19$, 20, and 21 vibrational levels of the deuterium singlet potential. The crosses are the physical bound states, while the circles denote the resonance energies, both at integer l values. The energies of the $l=6$ and 7 resonances that follow from Fig. 4 are in agreement with the position of the $l=6$ and 7 resonances, visible in Fig. 3. The above-mentioned three $l=6$ resonances are a manifestation of a single singlet resonance, but are shifted according to the energies at which various scattering channels contributing to λ_2 are in resonance. The three $l=7$ resonances overlap completely and are not separately visible, as their width is much larger than the hyperfine splitting. From Fig. 4 it also seems plausible that the broad structure for the $l=2$ partial wave between 2 and 5 K is a resonance related to the $v=21$ trajectory. In both the total $\lambda_2(E)$ and $\lambda_4(E)$ curves in Fig. 2 this structure is visible as a "wiggle" in the same energy interval.

In Figs. 5 and 6 the CC results for the $\bar{\lambda}$ and $\bar{\sigma}$ quanti-

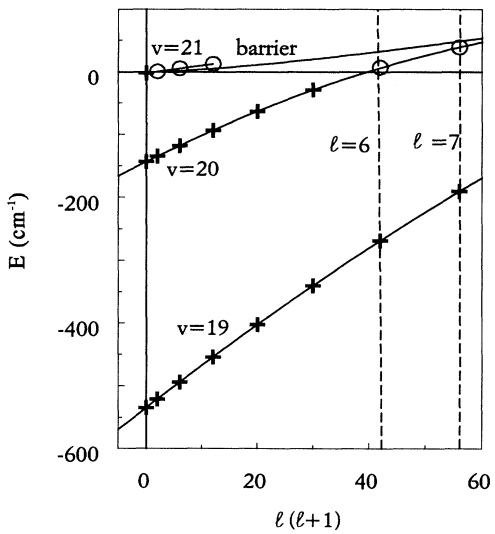

FIG. 4. "Trajectories" of vibrational levels $v=19$, 20, and 21 of the singlet potential in the E-vs-$l(l+1)$ plane. The crosses denote bound states and the circles denote resonances both at integer (physical) values of l. The line indicated by "barrier" shows approximately the height of the centrifugal barrier for a given l. The exact abscissas for $l=6$ and 7 are indicated by the dashed lines.

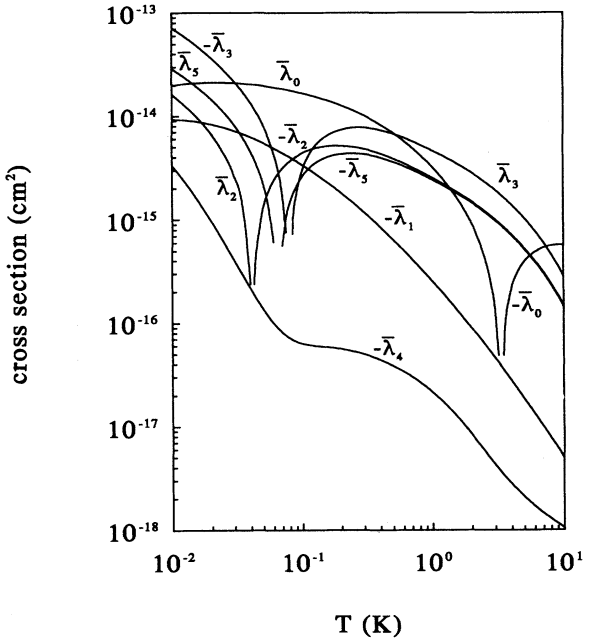

FIG. 5. Thermally averaged frequency-shift cross sections $\bar{\lambda}_i$ of the β-ϵ maser at $B=3.0\ \mu$T as a function of temperature.

ties as a function of temperature are given. For temperatures $T<10$ K integration over energies up to 100 K and partial waves $l\leq 8$ are necessary. After thermal averaging the resonances are no longer visible and the cusps due to threshold effects also disappear, except for a weak bend in λ_2 at $T=30$ mK, i.e., equal to twice the hyperfine splitting.

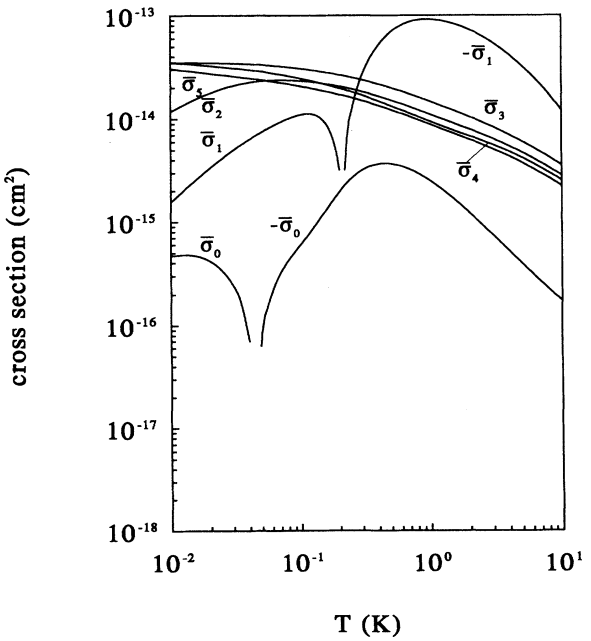

FIG. 6. Thermally averaged line-broadening cross sections $\bar{\sigma}_i$ of the β-ϵ maser at $B=3.0\ \mu$T as a function of temperature.

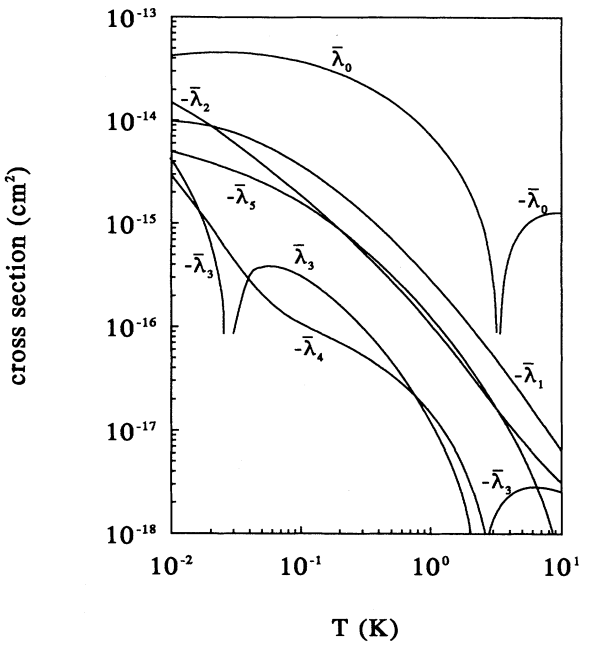

FIG. 7. Thermally averaged frequency-shift cross sections $\bar{\lambda}_i$ of the β-δ maser at $B=3.9$ mT as a function of temperature.

IV. THE β-δ MASER

The frequency shift of this maser is again rewritten:

$$\Delta\omega_c = n\langle v\rangle_{\rm th}[\bar{\lambda}_0(\rho_{\delta\delta}-\rho_{\beta\beta})+\bar{\lambda}_1(\rho_{\delta\delta}+\rho_{\beta\beta}) +\bar{\lambda}_2\rho_{\alpha\alpha}+\bar{\lambda}_3\rho_{\gamma\gamma}+\bar{\lambda}_4\rho_{\epsilon\epsilon}+\bar{\lambda}_5\rho_{\zeta\zeta}]\ , \qquad (11)$$

with a corresponding expression for the line broadening Γ_c with λ_i replaced by σ_i. The nonaveraged cross sec-

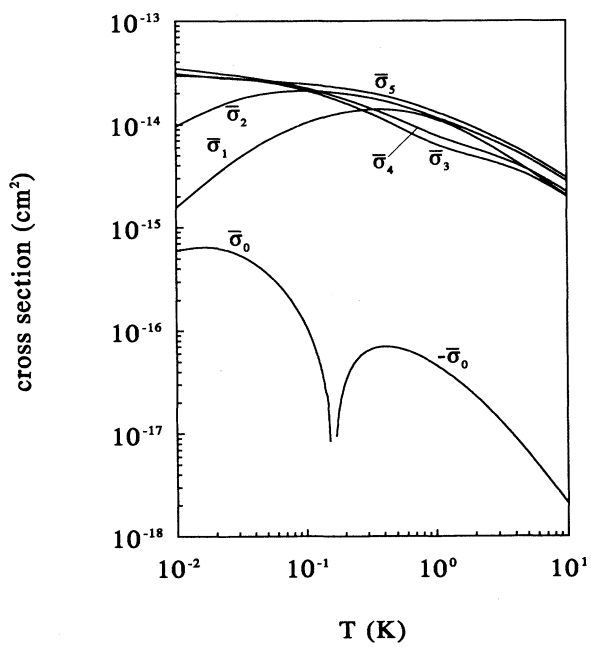

FIG. 8. Thermally averaged line-broadening cross sections $\bar{\sigma}_i$ of the β-δ maser at $B=3.9$ mT as a function of temperature.

tions λ_i and σ_i show cusps and resonances with the same origin as for the β-ϵ maser. Again, they disappear after thermal averaging. In Figs. 7 and 8 the cross sections $\bar{\lambda}_i$ and $\bar{\sigma}_i$ as a function of temperature are shown. For temperatures above twice the hyperfine splitting, the cross sections λ_i with $i=1,\ldots,5$ are smaller than $\bar{\lambda}_0$ by several orders of magnitude. This can be understood on the basis of the DIS approximation, which is valid at these temperatures. It predicts $\lambda_i^{\mathrm{DIS}}=0$ if $i=1,\ldots,5$ for the same (symmetry) reason, explaining the vanishing λ_1 and λ_2 cross sections of the H maser at zero magnetic field [16,17].

V. CONCLUSIONS

The approximate results on the basis of the DIS approximation plus first-order corrections given in our preliminary report for the β-ϵ maser are confirmed by the rigorous CC calculations of the present paper. Before summation over partial waves and thermal averaging, the calculated cross sections show pronounced resonance structures, which can be explained in terms of resonances in singlet elastic scattering. Even after summation over l, the energy dependence of the cross sections shows cusp structures related to the passage of thresholds in the various scattering channels.

In the case of the β-δ maser, the DIS approximation predicts that λ_0 is the only nonvanishing frequency-shift cross section. The rigorous CC results show a corresponding strong dominance of $\bar{\lambda}_0$ relative to the remaining $\bar{\lambda}_i$ quantities. The values of the latter are certainly substantial, however, and do provide a potential testing ground for theoretical predictions of collisional frequency shifts. The cusp and resonance structures occurring in the energy-dependent cross sections again disappear after thermal averaging.

ACKNOWLEDGMENT

This work is part of a research program of the Stichting voor Fundamenteel Onderzoek der Materie, which is financially supported by the Nederlandse Organisatie voor Wetenschappelijk Onderzoek.

[1] H. M. Goldenberg, D. Kleppner, and N. F. Ramsey, Phys. Rev. Lett. **5**, 361 (1960).
[2] B. S. Mathur, S. B. Crampton, D. Kleppner, and N. F. Ramsey, Phys. Rev. **158**, 14 (1967).
[3] D. J. Wineland and N. F. Ramsey, Phys. Rev. A **5**, 821 (1972).
[4] For reviews, see C. Audoin and J. P. Schermann, *Advances in Atomic and Molecular Physics* (Academic, New York, 1971), Vol. 7; J. Vanier and C. Audoin, *The Quantum Physics of Atomic Frequency Standards* (Hilger, Philadelphia, 1989), Chap. 6.
[5] M. W. Reynolds, Ph.D. thesis, University of British Columbia, 1989 (unpublished).
[6] M. E. Hayden, Ph.D thesis, University of British Columbia, 1991 (unpublished).
[7] M. E. Hayden, M. W. Reynolds, and W. N. Hardy, Physica B **169**, 541 (1991).
[8] S. B. Crampton, Ann. Phys. (Paris) **10**, 893 (1985).
[9] H. F. Hess, G. P. Kochanski, J. M. Doyle, T. J. Greytak, and D. Kleppner, Phys. Rev. A **34**, 1602 (1986).
[10] R. L. Walsworth, I. F. Silvera, H. P. Godfried, C. C. Agosta, R. F. C. Vessot, and E. M. Mattison, Phys. Rev. A **34**, 2550 (1986).
[11] E. M. Purcell and G. B. Field, Astrophys. J **124**, 542 (1956).
[12] J. P. Wittke and R. H. Dicke, Phys. Rev. **103**, 620 (1956).
[13] A. Dalgarno, Proc. R. Soc. London, Ser. A **262**, 132 (1961).
[14] P. L. Bender, Phys. Rev. **132**, 2154 (1963).
[15] L. C. Balling, R. J. Hanson, and F. M. Pipkin, Phys. Rev. **133**, A607 (1964); **135**, AB1 (1964).
[16] B. J. Verhaar, J. M. V. A. Koelman, H. T. C. Stoof, O. J. Luiten, and S. B. Crampton, Phys. Rev. A **35**, 3825 (1987).
[17] J. M. V. A. Koelman, S. B. Crampton, H. T. C. Stoof, O. J. Luiten, and B. J. Verhaar, Phys. Rev. A **38**, 3535 (1988).
[18] S. B. Crampton, Phys. Rev. **158**, 57 (1967).
[19] S. B. Crampton and H. T. M. Wang, Phys. Rev. A **12**, 1305 (1975).
[20] R. L. Walsworth, I. F. Silvera, E. M. Mattison, and R. F. C. Vessot, Phys. Rev. A **46**, 2495 (1992).
[21] E. Tiesinga, H. T. C. Stoof, B. J. Verhaar, and S. B. Crampton, Physica B **165&166**, 19 (1990).
[22] C. Schwartz and R. J. Le Roy, J. Mol. Spectrosc. **121**, 420 (1987).
[23] W. Kolos, K. Szalewicz, and H. J. Monkhorst, J. Chem. Phys. **84**, 3278 (1986).
[24] A. M. Schulte and B. J. Verhaar, Nucl. Phys. A **232**, 215 (1974).
[25] M. Bijlsma, B. J. Verhaar, and D. J. Heinzen (unpublished).
[26] E. Tiesinga, S. J. M. Kuppens, B. J. Verhaar, and H. T. C. Stoof, Phys. Rev. A **43**, 5188 (1991).
[27] R. G. Newton, *Scattering Theory of Waves and Particles* (Springer-Verlag, New York, 1982).
[28] V. de Alfaro, and T. Regge, *Potential Scattering* (North-Holland, Amsterdam, 1965).
[29] T. G. Weach and R. B. Bernstein, J. Chem. Phys. **46**, 4905 (1967).